Acta Pharmaceutica Sinica B 2024;14(11):5074−5078

Chinese Pharmaceutical Association
Institute of Materia Medica, Chinese Academy of Medical Sciences

Acta Pharmaceutica Sinica B

www.elsevier.com/locate/apsb
www.sciencedirect.com

LETTER TO THE EDITOR

Systemic and dynamic immune landscape of Omicron-infected subjects treated with Lianhua Qingwen capsules

KEY WORDS

COVID-19;
LHQW capsule;
Chinese traditional medicine;
Immune landscape

To the Editor:

The COVID-19 has represented an unexpected global public health challenge due to the profound immune evasion and transmission capabilities of the responsible virus SARS-CoV-2[1], being in great short of effective prophylactic and curative methods. Lianhua Qingwen (LHQW) capsule, a traditional Chinese medicine (TCM) formula, is officially included in China's COVID-19 treatment guidelines and has shown antiviral activity *in vitro* and *in vivo*. Recent clinical trials have shown that LHQW can alleviate symptoms and accelerate recovery in Omicron-infected patients[2]. The immune pathology of COVID-19 involves a complex interplay between virus-induced injuries and multifactorial immune responses. However, a comprehensive analysis of the immunological basis of LHQW's effects in Omicron-infected subjects is still lacking.

In an open-label randomized controlled study, we integrated immunophenotyping, transcriptomics, and plasma cytokine profiles of 41 COVID-19 patients over two weeks of LHQW administration or control treatment from symptom onset. Our findings reveal the systemic and dynamic alterations of innate and adaptive immune responses, providing insights into the phase-dependent immunomodulatory effects of LHQW.

1. Clinical parameters of LHQW-treated COVID-19 patients

To investigate the influence of LHQW capsules on immunological responses in Omicron-infected COVID-19 patients, we conducted an open-label, randomized controlled study at the Third People's Hospital of Shenzhen, China, 2022. Participants aged 18−59 years with balanced distributions across sex, BMI, race, smoking habits, and alcohol consumption were selected, excluding those with comorbidities. Forty-one patients with mild COVID-19 symptoms were enrolled and randomly divided into the LHQW group and control group at a ratio of 2:1. The LHQW group (26 patients) received a combination of LHQW capsules and vitamin C (VitC), while the control group (15 patients) received VitC only. Twenty healthy volunteers were also included for comparative analysis (Fig. 1A and Supporting Information Tables S1 and S2). Peripheral blood mononuclear cells (PBMCs) were analyzed using mass cytometry (CyTOF) and RNA sequencing (RNA-seq) at three time points: before treatment (V1), on Day 7 ± 1 of hospitalization (V2), and on Day 14 ± 2 of hospitalization (V3). Plasma proteins were concurrently examined using Olink proteomics. Meanwhile, clinical symptoms including fever, cough, shortness of breath, and fatigue were closely monitored. Interestingly, the symptom recovery rate from Day 7 to Day 14 was significantly higher in the LHQW group compared to the control group (Supporting Information Fig. S1).

2. LHQW treatment modulates T cell activation and exhaustion in a phase-dependent manner

Using a customized panel of 39 surface markers, we conducted comprehensive analyses with t-SNE and FlowSOM, identifying 43

Peer review under the responsibility of Chinese Pharmaceutical Association and Institute of Materia Medica, Chinese Academy of Medical Sciences.

https://doi.org/10.1016/j.apsb.2024.09.011

distinct immune cell clusters (Fig. 1B and Supporting Information Fig. S2, Tables S3 and S4). These clusters included 4 B cell subsets, 28 $CD3^+$ T cell subsets, 6 NK cell subsets, 2 dendritic cell (DC) subsets, 2 monocyte subsets, and 1 pre-neutrophil subset. Utilizing seven cell surface markers (CD45RA, CD45RO, CD62L, CCR7, CD95, CD25, and CD127), we identified 14 $CD4^+$ T cell clusters: naïve (T11-T12), naïve-like (T06-T08), central memory (T18), effector memory (T19-23), Tregs (T09, T17), and an unclassified subset (T10) (Fig. 1C and Supporting Information Fig. S3A). While the frequency of memory Tregs (T17) remained unchanged at V1, it significantly decreased after one week of LHQW treatment at V2 (Fig. 1C), indicating that LHQW treatment might suppress pathogenic memory Treg maintenance.

Subsequently, using seven surface markers (CD45RA, CD45RO, CD62L, CCR7, CD95, CD57, and CD161), we identified nine distinct $CD8^+$ T cell subsets, including naïve (T02-T03), naïve-like (T04-T05), effector memory (T15-T16), effector (T27), exhausted (T26), and mucosal-associated invariant T (MAIT) cells (T14) (Fig. 1D and Fig. S3B). Notably, the frequency of $CD28^{int}CD127^{int}$ naïve-like $CD8^+$ T cells (T04) increased after infection and significantly further increased after one week of LHQW treatment compared to the control group (Fig. 1D), suggesting a potential promotion of early $CD8^+$ T cell activation by LHQW. Moreover, after two weeks of treatment (at V3), the frequency of exhausted $CD8^+$ T cells (T26) significantly decreased in the LHQW group compared to the control group, implying that LHQW may help in mitigating $CD8^+$ T cell exhaustion (Fig. 1D). Nevertheless, the $\gamma\delta$ T cell subsets were unaffected by LHQW treatment (Fig. S3C).

In NK cell analysis, six subsets (NK01-NK06) were identified (Fig. 1E and Fig. S3D). Pseudotime analysis revealed NK cells polarized into two ends: immature (NK01 and NK02) and mature (NK06). $CD56^{int}CD16^{hi}CD161^{hi}CD57^-$ NK cells (NK03) were in an intermediate state between NK01/NK02 and NK06, being corroborated by the absence of CD57 in NK03, a marker of NK cell maturation[3] (Fig. S3E). Interestingly, NK03 frequency decreased specifically after one week of LHQW treatment (Fig. 1E), while other NK subsets remained unchanged. Overall, these results imply that LHQW administration may suppress the maintenance of memory Tregs and immature NK cells while enhancing the early activation of $CD8^+$ T cells after one week, being followed by a reduction in exhausted $CD8^+$ T cells after two weeks.

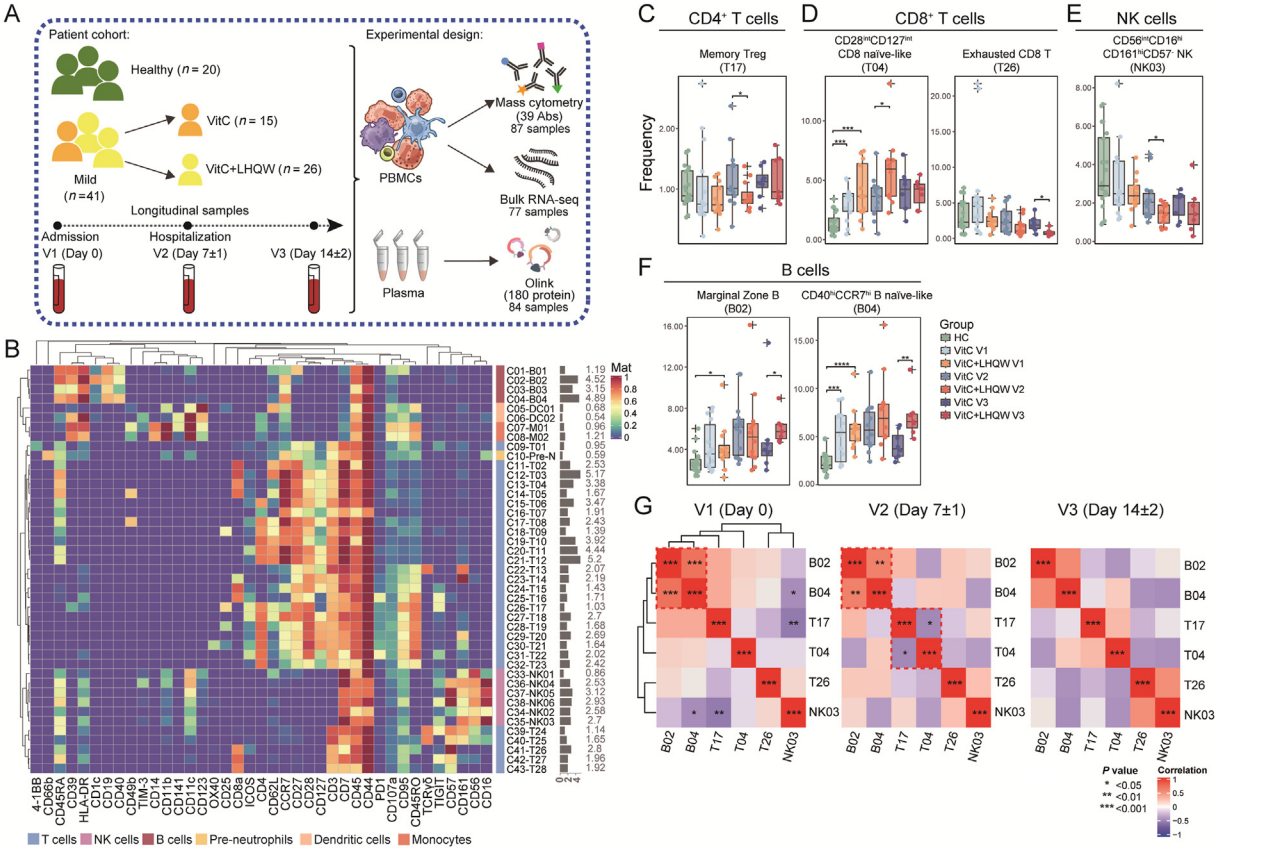

Figure 1 Study design and lymphocytic compartment measurement. (A) Study design. Cohort of mild Omicron-infected subjects treated with vitamin C (VitC) or VitC+LHQW capsules. PBMCs were analyzed by CyTOF and RNA-seq; plasma proteins were quantified by Olink. (B) Heatmap showing normalized marker expression for 43 clusters identified with FlowSOM. Bar graph to the right shows relative frequencies. (C−F) Boxplots of $CD4^+$ T cell clusters (C), $CD8^+$ T cell clusters (D), NK cell clusters (E), and B cell clusters (F). (G) Heatmap of Spearman correlations for immune cell cluster frequencies in samples taken at V1 (Day 0) (left), V2 (Day 7 ± 1) (middle), and V3 (Day 14 ± 2) (right). Box plots represent the interquartile range (IQR), with the horizontal line indicating the median (n = 7−20). Whiskers extend to the farthest data point within a maximum of 1.5 × IQR. In (C−F), significance was determined by unpaired Wilcoxon test. *P < 0.05, **P < 0.01, ***P < 0.001.

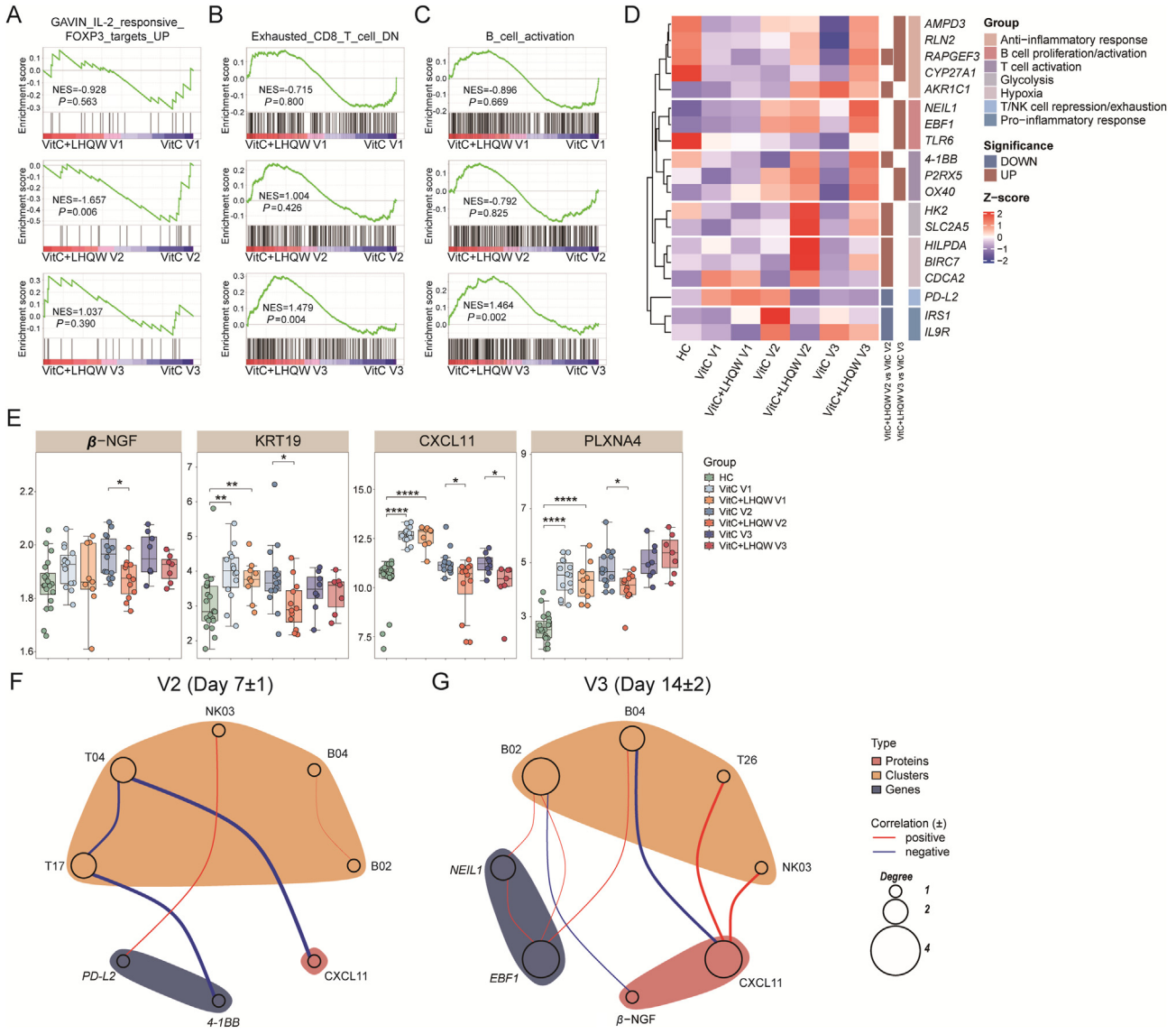

Figure 2 An immune signature composite is altered over time. (A−C) GSEA of enrichment profiles differentially expressed between VitC+LHQW and VitC in PBMCs at V1 (upper), V2 (middle), or V3 (bottom) using FOXP3 targets (A), exhausted $CD8^+$ T cell downregulated signature (B), and B cell activation signature (C). (D) Heatmap of selected genes differentially expressed between VitC+LHQW and VitC in PBMCs at V2 or V3. Upregulated genes in red, downregulated genes in blue (fold change $\geq$1.5, $P < 0.05$). (E) Boxplots of plasma cytokines significantly different between VitC+LHQW and VitC in samples taken at V2 or V3. (F−G) Correlation-based network of 6 immune cell clusters, 4 genes, and 2 cytokines in samples taken at V2 (F) and V3 (G). Each edge represents a significant correlation ($P < 0.05$, $|R| > 0.3$). Edge widths proportional to correlation coefficient; red for positive, blue for negative correlations. Node size proportional to degree centrality. Box plots represent the interquartile range (IQR), with the horizontal line indicating the median (n = 7−20). Whiskers extend to the farthest data point within a maximum of 1.5 × IQR. In (E), significance was determined by unpaired Wilcoxon test. *$P < 0.05$, **$P < 0.01$, ***$P < 0.001$, ****$P < 0.0001$.

3. LHQW treatment increases innate B cell numbers and stimulates B cell activation in COVID-19 patients

In the analysis of B cells, we identified four subsets: marginal zone B Cells (MZB, B02), $CD40^{lo}CCR7^{int}$ naïve B cells (B03), $CD40^{hi}CCR7^{hi}$ naïve-like B cells (B04) and memory B cells (B01) (Fig. 1F and Fig. S3F). Notably, the frequencies of the B02 and B04 was increased after infection. The MZB cells (B02), known for their role in the innate immune response and rapid antibody production[4], showed a marked increase in frequency after two weeks of LHQW treatment in the LHQW group compared to the control group (Fig. 1F). Meanwhile, the frequency of $CD40^{hi}CCR7^{hi}$ naïve-like B cells (B04) was also dramatically increased in the LHQW group compared with the control group (Fig. 1F). Given the critical role of CCR7 in activating humoral immunity[5], our findings suggest that two weeks of LHQW treatment may promote B cell activation.

Next, we analyzed the frequencies of innate myeloid immune cell subsets. However, none of these were significantly affected by LHQW (Supporting Information Fig. S4), suggesting that LHQW

treatment may selectively target lymphoid rather than myeloid cells.

To explore the associations among lymphocyte responses to LHQW, we performed pairwise Spearman correlation analyses on six immune subsets whose frequencies were significantly altered after LHQW treatment in COVID-19 patients. A strong positive correlation was found between $CD40^{hi}CCR7^{hi}$ naïve-like B cells (B04) and MZB cells (B02) before and after LHQW treatment (Fig. 1G), confirming LHQW's role of the humoral immune response. Conversely, a negative correlation was observed between immunosuppressive memory Tregs (T17) and potential immunocompetent naïve-like $CD8^+$ T cells (T04) after one week of LHQW treatment (Fig. 1G). This suggests LHQW's capacity to reduce immunosuppression while enhancing cellular immunity, which is critical for restricting viral infections.

4. LHQW treatment shows early Treg reduction and subsequent B cell activation with reduced $CD8^+$ T cell exhaustion

To better understand the molecular mechanisms behind immunological changes following LHQW treatment, we conducted RNA-seq on individual PBMC samples across the same cohorts. Gene set enrichment analysis (GSEA) identified several key regulatory pathways, including Treg transcriptional regulation and $CD8^+$ T cell exhaustion, which were more active in the control group than in the LHQW group at the V2 or V3 time points (Fig. 2A and B), mirroring CyTOF analysis. Conversely, glycolysis and hypoxia metabolism pathways were more active in the LHQW group at V2, suggesting a metabolic feature of enhanced lymphocytic activation (Supporting Information Fig. S5A and S5B). Additionally, B cell activation and anti-inflammatory pathways were positively associated with the LHQW group after two weeks of treatment at V3, but not at V1 or V2 (Fig. 2C and Fig. S5C).

A deeper dive into these gene sets revealed a shift towards anti-inflammatory responses driven by LHQW. This is indicated by the upregulation of anti-inflammatory genes and downregulation of pro-inflammatory genes in the LHQW group (Fig. 2D). Genes linked to B cell proliferation and activation (*NEIL1*, *EBF1*, *TLR6*) and T cell activation (*4-1BB*, *P2RX5*, and *OX40*) were upregulated in the LHQW group, while *PD-L2*, a gene involved in T and NK cell exhaustion, was downregulated (Fig. 2D). These findings suggest that LHQW protects lymphocyte functionality by limiting over-activation. Upregulation of genes also involved in glycolysis and hypoxia pathways (Fig. 2D), indicating metabolic reprogramming and enhanced lymphocyte function post-LHQW treatment. In summary, LHQW treatment in COVID-19 patients promotes early $CD8^+$ T cell activation and reduces Tregs at V2, while mitigating inflammation, reducing $CD8^+$ T cell exhaustion, and promoting B cell activation at V3. This supports LHQW as a beneficial intervention for COVID-19.

Next, we evaluated inflammatory proteins in plasma using the Olink proteomic assay. Among them, β-NGF and KRT19, potential biomarkers for predicting adverse COVID-19 outcomes, showed significant reductions in the LHQW group after one week of treatment (Fig. 2E). Moreover, CXCL11, which recruits Treg to attenuate T cell and NK cell activation, significantly reduced in the LHQW group over one and two weeks. PLXNA4, an immune checkpoint inhibitor that negatively regulates T cell activation, also decreased after a week of LHQW treatment (Fig. 2E). These protein changes align with the observed cellular dynamics.

5. Prolonged LHQW treatment shifts immunological focus from T cell activation to B cell activation

We performed correlation-based network analysis on six immune cell clusters (T17, T04, T26, NK03, B02, and B04), four genes (*4-1BB*, *PD-L2*, *EBF1*, and *NEIL1*), and two plasma proteins (CXCL11 and β-NGF) differentially expressed between the LHQW and control groups at V2 and V3. At V2, revealing that the correlations between memory Tregs (T17) and naïve-like $CD8^+$ T cells (T04) and between two B cell subsets were predominant (Fig. 2F). The strongest correlations were between CXCL11 levels and T04 frequency, and *4-1BB* mRNA levels and T17 frequency, with a milder positive correlation exists between PD-L2 and NK03. These results suggest that LHQW's initial immunological regulation focuses on T cell activation. By V3, correlations between CXCL11 and B04, T26, and NK03 were predominant, along with additional correlations between B02 or B04 and *NEIL1* or *EBF1* (Fig. 2G). The increased presence of B02 and B04 at V3 highlights a shift of LHQW regulatory effects towards B cell activation in the second week of treatment. These results indicate that LHQW creates a dynamic immunological landscape, initially marked by early T cell activation and later by enhanced B cell activation, supporting its potential as a strategic intervention to accelerate symptom recovery in COVID-19 patients.

Acknowledgments

We thank the patients and blood donors, their families and medical personnel. We thank Hui Liang and Chuan Shan from Standard BioTools for technical assistance. This work was supported by the Key Project of National Natural Science Foundation of China (82130123), the Innovation Team and Talents Cultivation Program of National Administration of Traditional Chinese Medicine (ZYYCXTD-D-202206, China).

Author contributions

Shijun Chen: Writing − original draft, Visualization, Methodology, Investigation, Formal analysis, Data curation. Fuxiang Wang: Resources, Formal analysis, Data curation. Yuanlong Lin: Resources, Formal analysis, Data curation. Yinyin Xie: Validation, Investigation. Ruihong Zhang: Validation, Investigation. Juan Chen: Validation, Investigation. Niu Qiao: Visualization, Resources, Formal analysis. Tong Yin: Visualization, Resources, Formal analysis. Yun Tan: Visualization, Formal analysis. Hai Fang: Visualization, Resources, Formal analysis. Hongzhou Lu: Resources, Formal analysis, Data curation. Zhu Chen: Writing − review & editing, Supervision. Shanhe Yu: Writing − review & editing, Writing − original draft, Supervision, Resources, Methodology, Investigation, Formal analysis, Data curation, Conceptualization. Jiang Zhu: Writing − review & editing, Supervision, Conceptualization. Zhenhua Jia: Writing − review & editing, Supervision, Funding acquisition. Saijuan Chen: Writing − review & editing, Supervision, Resources, Project administration, Conceptualization.

Conflicts of interest

Shijiazhuang Yiling Pharmaceutical Co., Ltd. provided the clinical research drug free of charge. Professor Jia Zhenhua is the spouse of Ms. Wu Rui, who holds shares in Shijiazhuang Yiling Pharmaceutical Co., Ltd. and serves as a director. The remaining authors declare no competing financial interests.

Appendix A. Supporting information

Supporting information to this article can be found online at https://doi.org/10.1016/j.apsb.2024.09.011.

References

1. Yu S, Lin Y, Li Y, Chen S, Zhou L, Song H, et al. Systemic immune profiling of Omicron-infected subjects inoculated with different doses of inactivated virus vaccine. *Cell* 2023;**186**:4615−31.e16.
2. Zheng JP, Ling Y, Jiang LS, Mootsikapun P, Lu HZ, Chayakulkeeree M, et al. Effects of Lianhuaqingwen Capsules in adults with mild-to-moderate coronavirus disease 2019: an international, multicenter, double-blind, randomized controlled trial. *Virol J* 2023;**20**:277.
3. Björkström NK, Ljunggren HG, Michaëlsson J. Emerging insights into natural killer cells in human peripheral tissues. *Nat Rev Immunol* 2016;**16**:310−20.
4. Cerutti A, Cols M, Puga I. Marginal zone B cells: virtues of innate-like antibody-producing lymphocytes. *Nat Rev Immunol* 2013;**13**:118−32.
5. Tokunaga R, Naseem M, Lo JH, Battaglin F, Soni S, Puccini A, et al. B cell and B cell-related pathways for novel cancer treatments. *Cancer Treat Rev* 2019;**73**:10−9.

Shijun Chen[a], Fuxiang Wang[b], Yuanlong Lin[b], Yinyin Xie[a], Ruihong Zhang[a], Juan Chen[a], Niu Qiao[a], Tong Yin[a], Yun Tan[a], Hai Fang[a], Hongzhou Lu[b], Zhu Chen[a], Shanhe Yu[a,*], Jiang Zhu[a,*], Zhenhua Jia[c,d,*], Saijuan Chen[a,*]

[a]*Shanghai Institute of Hematology, State Key Laboratory of Medical Genomics, National Research Center for Translational Medicine at Shanghai, Collaborative Innovation Center of Hematology, Ruijin Hospital Affiliated to Shanghai Jiao Tong University School of Medicine, Shanghai 200025, China*

[b]*Department of Infectious Diseases, National Clinical Research Centre for Infectious Diseases, the Third People's Hospital of Shenzhen and the Second Affiliated Hospital of Southern University of Science and Technology, Shenzhen 518112, China*

[c]*Hebei Academy of Integrated Traditional Chinese and Western Medicine, Shijiazhuang 050035, China*

[d]*National Key Laboratory for Innovation and Transformation of Luobing Theory, Shijiazhuang 050035, China*

*Corresponding authors.
E-mail addresses: yushanhe5460@163.com (Shanhe Yu), zhujiang@shsmu.edu.cn (Jiang Zhu), jzhjiazhenhua@163.com (Zhenhua Jia), sjchen@stn.sh.cn (Saijuan Chen)

Received 26 June 2024
Received in revised form 16 July 2024
Accepted 5 August 2024